SiF 2022– The 12th International Conference on Structures in Fire
The Hong Kong Polytechnic University, Nov 30 - Dec 2, 2022

FIRES FOLLOWING EARTHQUAKE FRAGILITY FUNCTIONS OF STEEL BRACED FRAMES

Patrick Covi[1], Nicola Tondini[2], Amir Sarreshtehdari[3], Negar Elhami-Khorasani[4]

ABSTRACT

The paper describes the outcomes of the analysis of a steel braced frame subjected to fires following earthquake (FFE). Nonlinear time-history analyses were performed in order to evaluate the seismic response. Then, based on the damage suffered by the structure, which was estimated according to the inter-storey drift ratio (IDR) and floor acceleration, the post-earthquake fire ignitions within selected compartments were considered. Natural fire curves were determined by means of zone models. Thus, compartmentation and opening characteristics were included in the analysis. Finally, thermomechanical analyses were run and failure criteria based on the column and beam displacement and rate of displacement were applied. The results of the probabilistic analyses were used to produce fragility functions to evaluate the probability of exceeding a limit state conditioned on an intensity measure in the context of FFE.

Keywords: Fire following earthquake; fragility functions; concentrically braced steel frames; probabilistic framework.

1 INTRODUCTION

The engineering design practice typically analyzes seismic and fire events independently. However, several historical events show that the consequences associated with fire following an earthquake (FFE) event can be significantly higher compared to the damages and losses caused by only the seismic event [1-2]. The 1906 San Francisco earthquake was one of the most significant FFE scenarios, in which fires destroyed around 80% of the city. Other major FFE events that occurred in the past include the Tokyo earthquake (1923), the Kobe earthquake (1995) and the Tohoku earthquake (2011).

Post-earthquake ignition sources identified from past earthquakes are reviewed by Botting (1998) [3]. Also, Scawthorn (1992) [4] discusses ignition sources and predicts post-earthquake ignition rates for typical buildings for different earthquake intensities. In brief, the principal ignition sources are overturning of electrical appliances, short-circuiting of electrical equipment, gas leakage from damaged equipment and pipework, and leakage of flammable fluids. Damaged gas equipment and pipes may cause spark and hold fuel to propagate the fire while electrical household appliances may initiate spark with interior furnishings and other flammable materials. Another major concern is the high potential for ignition as electricity and gas supplies are restored some time after the earthquake. Leaking gas and damaged electrical appliances were identified as initiating fires in the days following the Kobe and Northridge earthquakes. An earthquake can lead to single or multiple ignitions in a building. In this context, the structural fire performance could be deteriorated because the fire acts on a previously damaged structure. The earthquake

[1] Postdoctoral Researcher, Department of Civil, Environmental and Mechanical Engineering, University of Trento (Italy)
e-mail: patrick.covi@unitn.it, ORCID: https://orcid.org/0000-0002-0570-4061
[2] Associate Professor, Department of Civil, Environmental and Mechanical Engineering, University of Trento (Italy)
e-mail: nicola.tondini@unitn.it, ORCID: https://orcid.org/0000-0003-2602-6121
[3] PhD Candidate, Department of Civil, Structural and Environmental Engineering, University at Buffalo (USA)
e-mail: amirsarr@buffalo.edu, ORCID: https://orcid.org/0000-0001-5630-2751
[4] Associate Professor, Department of Civil, Structural and Environmental Engineering, University at Buffalo (USA)
e-mail: negarkho@buffalo.edu, ORCID: https://orcid.org/0000-0003-3228-0097

may damage fire protection elements and the compartment measures with the consequence that the fire can spread more rapidly. Moreover, it is harder to control post-earthquake fires as there can be multiple ignitions across a community at once as well as possible disruptions within the infrastructure networks, such as water supply system, that hinder timely intervention [1].

2 FFE FRAMEWORK

The major steps for implementing the FFE probabilistic framework [5] are illustrated in Figure 1. The process is followed to perform probabilistic FFE analyses and to obtain sufficient data to build fragility curves and surfaces. The framework is developed and implemented using a combination of different software, i.e. OpenSees [6,7], Ozone [8], and MATLAB [10]. The seismic analyses and the FFE structural analyses were performed in OpenSees. The zone model software Ozone [8] was used for the fire development analyses, whereas a specific code developed in MATLAB was exploited for the heat transfer analyses.

The geometry of the structural system, cross section sizes, material properties, and applied loads are first defined in a Tcl script. Probabilistic parameters required for the analysis, such as compartment properties, are next generated. Once all the inputs and random variables are defined, the gravity and seismic analyses are performed. Then, OpenSees enters a "standby mode" and a background MATLAB process executes the FFE decision algorithm to automatically generate fire scenarios based on the seismic analysis results, in which the temperature of the hot gases in the compartments is computed using Ozone. Heat transfer is then conducted in MATLAB, followed by the structural analysis at elevated temperatures in OpenSees. Finally, the generated results are used to construct the fragility functions.

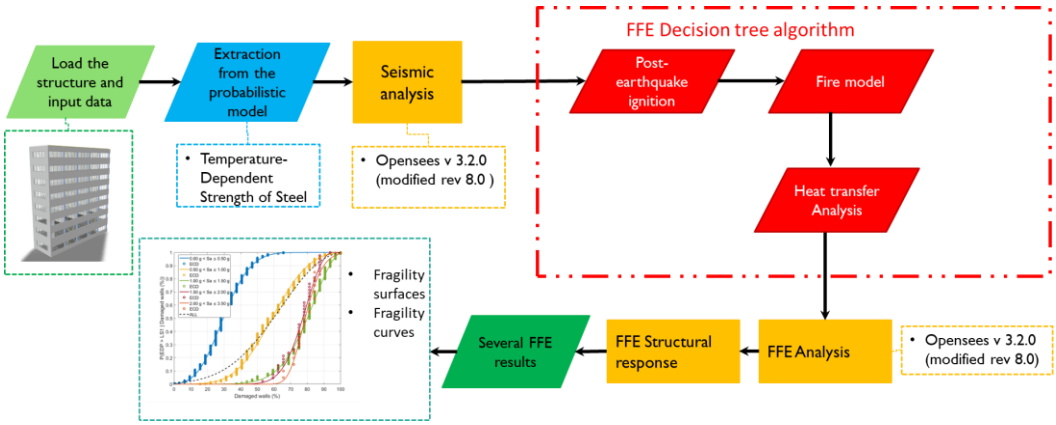

Figure 1. Major steps in the implemented FFE framework

The status of a compartment after an earthquake is based on the combined conditions of the glazing, partition walls, and doors and it is quantified using the fragility functions provided in FEMA P58 [9] background documentation.

The framework determines the possible damage of each compartment (glazing and wall damages) and generates the fire scenario based on the earthquake using the following three thresholds:

- The peak floor acceleration (PFA) of at least one floor must be greater than or equal to 0.7 g, this value corresponds to the 100% probability of exceeding breakage in gas pipe joints according to the fragility curves reported in Ueno et al., (2004) [11].
- The inter-story drift ratio (IDR) of the same floor must be greater than or equal to 1.0 %. This ignition criterion considers the possibility of having some damage to the electric cables that can be characterized as a function of the IDR. According to the FEMA P-356 (2000) [12], the requirements for life safety and collapse prevention performance levels for a steel braced frame structure are 0.5% and 2%, respectively. Therefore, the ignition criterion for a steel braced frame was assumed as 1% IDR, a value in between the two thresholds.

- The maximum IDR must remain below 6%. An IDR equal to 6% was chosen as the threshold for collapse, which is three times the recommended collapse limit state value for a braced steel frame (i.e., 2% IDR) in FEMA P-356 [12]. Extensive yielding, buckling of braces, and connection failure, are expected during the earthquake without the subsequent FFE event.

The yield strength of steel f_y at ambient (seismic analysis) and high temperatures (fire analysis) was modelled as a random variable using a continuous logistic function [13,14] (see Equation 1).

$$k_{y,2\%,T}=\frac{1.7\times\exp\left[\text{logit}\left(\hat{k}^{*}_{y,2\%,T}\right)+0.412-0.81\times10^{-3}\times T+0.58\times10^{-6}\times T^{1.9}+0.43\times\varepsilon\right]}{\exp\left[\text{logit}\left(\hat{k}^{*}_{y,2\%,T}\right)+0.412-0.81\times10^{-3}\times T+0.58\times10^{-6}\times T^{1.9}+0.43\times\varepsilon\right]+1} \quad (1)$$

where $\text{logit}\left(\hat{k}^{*}_{y,2\%,T}\right)=\ln\left(\frac{\hat{k}^{*}_{y,2\%,T}}{1-\hat{k}^{*}_{y,2\%,T}}\right)$, $\hat{k}^{*}_{y,2\%,T}=\frac{\hat{k}_{y,2\%,T}+10^{-6}}{1.7}$, and $\hat{k}_{y,2\%,T}$ is the temperature-specific retention factor as prescribed by EN1993-1-2 [20].

A custom material class, i.e., SteelFFEThermal, was developed for nonlinear FFE analyses in OpenSees. The SteelFFEThermal material has the same definition as the Giuffrè-Menegotto-Pinto uniaxial steel stress-strain model at ambient temperature. However, when the temperature is applied, the material class switches the constitutive law to the stress-strain constitutive law for steel at elevated temperature as for EN 1993-1-2 [22]. For a detailed description of how the FFE probabilistic framework was developed, the reader is referred to the thesis of Covi [5].

3 CASE STUDY

An eight-story three-bay steel frame with concentric bracings in two central bays was selected as a case study, as illustrated in Figure 2. The structure is an office building designed and presented in NIST Technical Note 1863-2 [15]. It is designed according to the ASCE 7-10 [16] recommendations for an area with high seismicity of the West coast of the United States; in particular, the city of Los Angeles was chosen for the case study location.

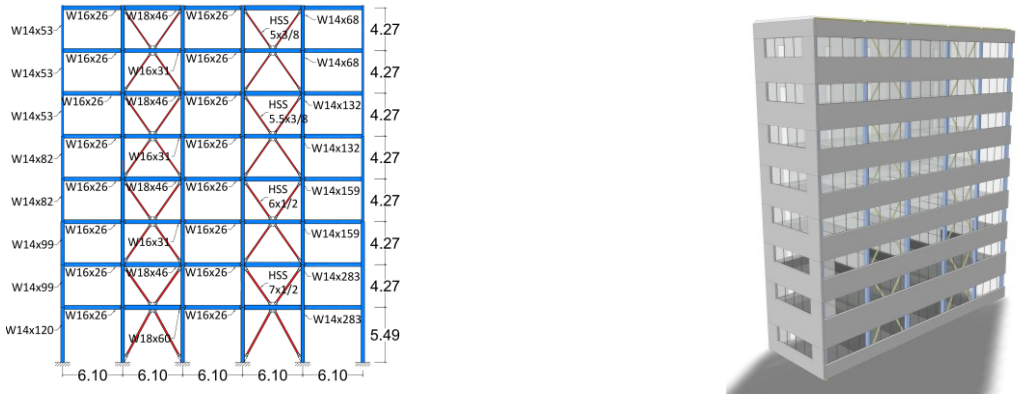

Figure 2. (a) Configuration of the frame (length in meters); (b) rendering of the building.

The building has a rectangular plan of 46.33 m in the E-W direction, including five 9.14 m bays, and 31.01 m in the N-S direction, including five 6.10 m bays. The story height is 4.28 m with the exception of the first floor, which is 5.49 m high. The width of the windows for the structure was varied from 1.5 to 6 m (5 to 20 ft) with 1.5 m (5 ft) intervals.

3.1 Ground motions

In order to perform non-linear time-history analyses, it was fundamental to model the seismic hazard through adequate selection and scaling of ground motion records. In this respect, a set of 14 accelerograms for the collapse limit state was selected from the FEMA P-695 dataset [17,18] considering the type of

spectrum, magnitude range, distance range, style-of-faulting, local site conditions, period range, and ground motion components using the PEER Ground Motion Database [19]. Table 1 summarizes the 14 strong motion records used for the N-S direction in the FFE analyses, including the magnitude and peak ground acceleration and the same ID numbering given in FEMA P-695 [17].

Accelerograms were modified to match the target spectrum in the period range of 0.3 to 2.25s that includes the fundamental period of the structure equal to 1.5 s. Figure 8 illustrates the set of acceleration response spectra, original and scaled, and the scaled average response spectrum. The accelerograms were used to perform the FFE probabilistic analysis and 6 scale factors were applied to the accelerograms: 0.50; 0.75; 1.00; 1.25; 1.50; 1.75.

Table 1. Accelerogram set.

ID	Event name	Station	Year	Mw	PGA (g)
1	Northridge, USA	Beverly Hills - Mulhol	1994	6.7	0.52
2	Northridge, USA	Canyon Country-WLC	1994	6.7	0.48
3	Duzce, Turkey	Bolu	1999	7.1	0.82
5	Imperial Valley, USA	Delta	1979	6.5	0.35
6	Imperial Valley, USA	El Centro Array #11	1979	6.5	0.38
8	Kobe, Japan	Shin-Osaka	1995	6.9	0.24
9	Kocaeli, Turkey	Duzce	1999	7.5	0.36
10	Kocaeli, Turkey	Arcelik	1999	7.5	0.22
11	Landers, USA	Yermo Fire Station	1992	7.3	0.24
14	Loma Prieta, USA	Gilroy Array #3	1989	6.9	0.56
16	Superstition Hills, USA	El Centro Imp. Co.	1987	6.5	0.36
17	Superstition Hills, USA	Poe Road (temp)	1987	6.5	0.45
18	Cape Mendocino, USA	Rio Dell Overpass	1992	7	0.55
19	Chi-Chi, Taiwan	CHY101	1999	7.6	0.44

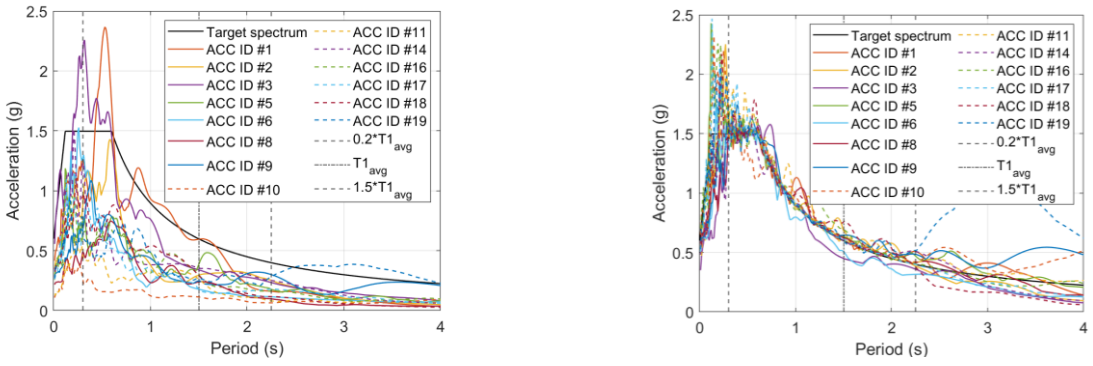

(a) (b)

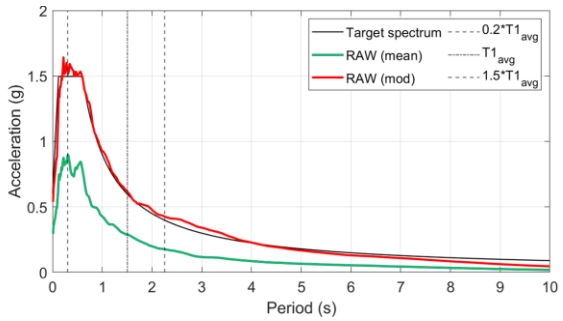

(c)

Figure 3. Acceleration Response Spectra: (a) original, (b) scaled, (c) scaled average spectrum.

3.2 Fire loads

Based on a discrete sampling uniform distribution, five values of fire load density were selected: i.e., 300 MJ/m^2; 600 MJ/m^2; 900 MJ/m^2; 1200 MJ/m^2; 1500 MJ/m^2. In the EN 1991-1-2 [20], an 80% fractile value of fire load density for office occupancies corresponds to 511 MJ/m^2 according to the Gumbel distribution. According to a recent survey conducted in the US, the measured total fire load density, including moveable and fixed content, had a mean value of 1486 MJ/m^2 [21]. For this reason, fire load density values up to 1500 MJ/m^2 were used and fire load density less than 300 MJ/m^2 was considered too low.

3.3 Finite element model

The frame was modelled with non-linear beam elements based on corotational formulation and the uniaxial SteelFFEThermal material was used for the braces, beams and columns. Geometric imperfections were included to allow for flexural buckling according to EN 1993-1-1 [23]. Masses were considered lumped at the floors, following the assumption of rigid diaphragms. Each column was discretized with four elements, while beam and brace elements were discretized using eight elements to get adequate precision in the calculation of displacements, stresses, and strains in sections of each member. Fiber sections were selected to define the cross section of the elements.

4 PROBABILISTIC ANALYSIS RESULTS

4.1 Earthquake simulation

For brevity, one sample simulation is selected as an example to demonstrate the methodology used for the FFE analyses. The selected seismic action is shown in Figure 12. The earthquake, known as the Landers earthquake, occurred at 4:57 am, June 28, 1992 with a magnitude of 7.3.

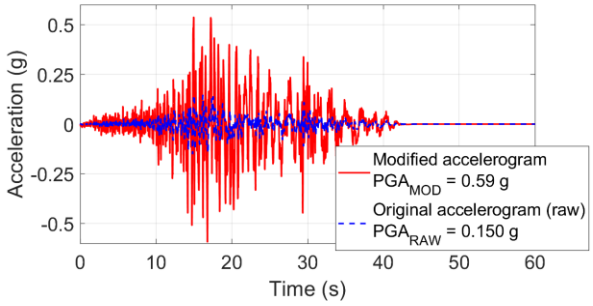

Figure 4. Comparison between the original and modified accelerogram for the FFE simulation.

Figure 5 illustrates the results of the numerical simulation of the non-linear dynamic analysis for the selected acceleration time-history. The energy dissipation was concentrated in the braces. All the columns and beams remained elastic during the seismic event.

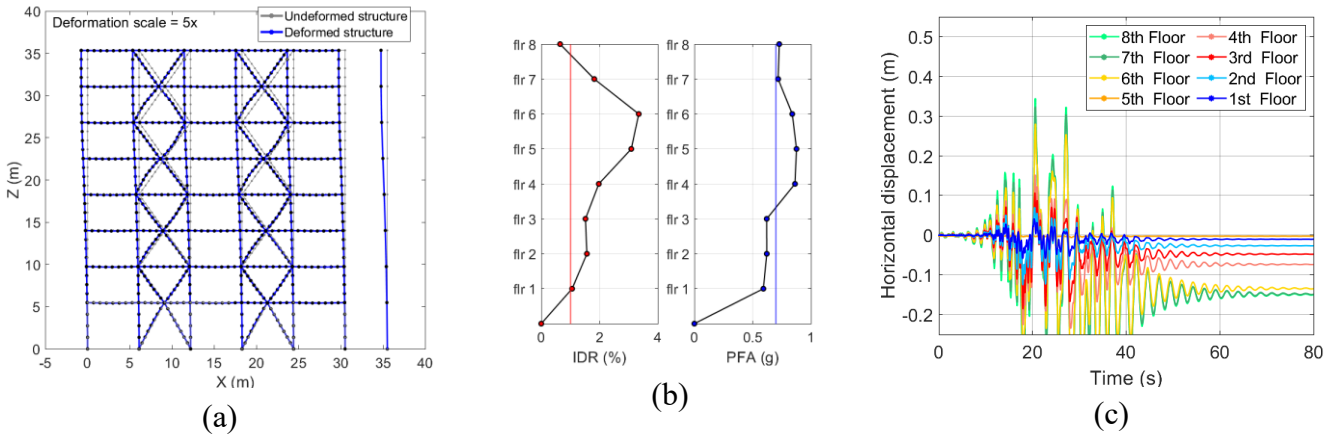

Figure 5. (a) Deformed shape at the end of the seismic event (amplified by a factor of 5); (b) maximum inter-story drift (IDR) and maximum peak floor acceleration (PFA); (c) horizontal displacement of the floors.

4.2 Post-earthquake fire simulation

The probabilistic FFE framework was used to automatically determine the possible damage to each compartment (glazing and wall damages) and generate the fire scenario based on the IDR and PFA thresholds. The framework includes the possibility to have the ignition in more than one compartment, due to multiple damage to the gas or electrical services or appliances in more than one location. For this reason, the framework could select more than one ignition after the earthquake. The flashover time is set as the threshold for the vertical spread between two exterior compartments. In the direction of the horizontal compartment, a delay time for the horizontal fire spreads of 30 minutes or 15 minutes was taken, depending on whether or not the partition remains intact after the earthquake event.

Figure 6a shows the evolution of the fire for the selected FFE scenario, Figure 6b illustrates the time-temperature curves for each compartment at 4th floor, while Figure 6c shows a qualitative representation of the compartment locations and dimensions for the selected case study.

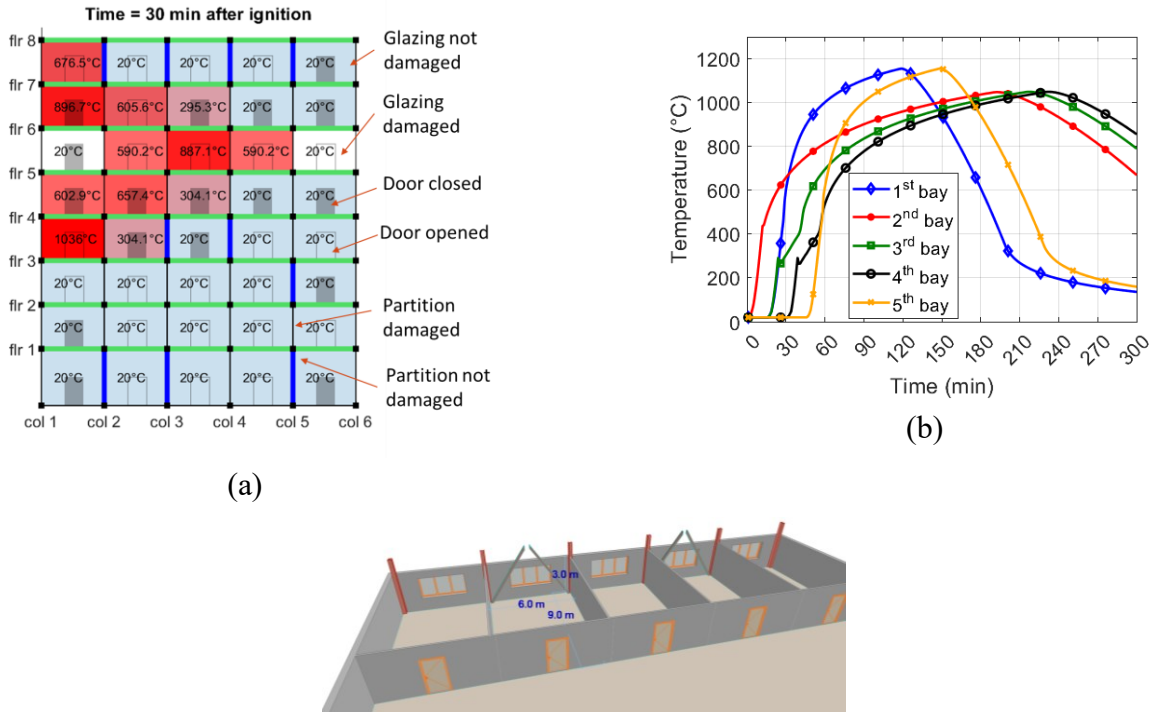

Figure 6. (a) Fire spread within the building after 30 minutes; (b) Time-temperature curve of fire for floor 4; (c) inside view of a compartment.

The time-temperature curve and characteristics of the fire behaviour in the compartments were quantified using Ozone. The heat transfer analysis was automatically performed to obtain steel temperatures for each element in the compartment subjected to fire using the probabilistic FFE framework.

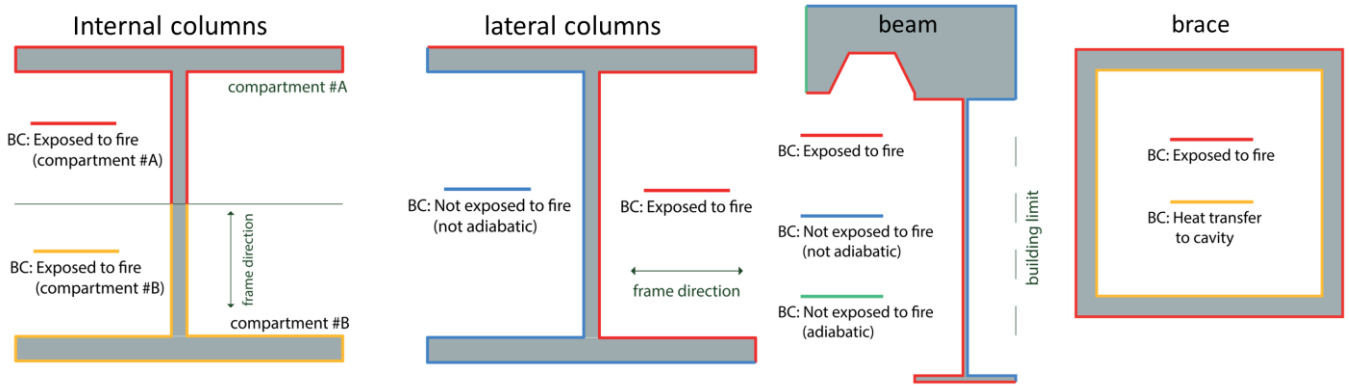

Figure 7: Boundary conditions for thermal analysis.

The FFE structural analysis followed the heat transfer analysis for the selected scenario. Structural partial collapse occurred 30 minutes after the start of the fire due to the excessive rate of vertical deflection in the beams located on the 4th and 7th floors and in the 1st bay, as illustrated in Figure 8a.

Figure 8b shows the final deformed configuration of the steel frame at the end of the simulation. In particular, despite the low utilization factor of the columns, the loss of transverse restraint owing to the beam failure caused an increase in the column effective length that eventually led to column buckling and the collapse of a portion of the building.

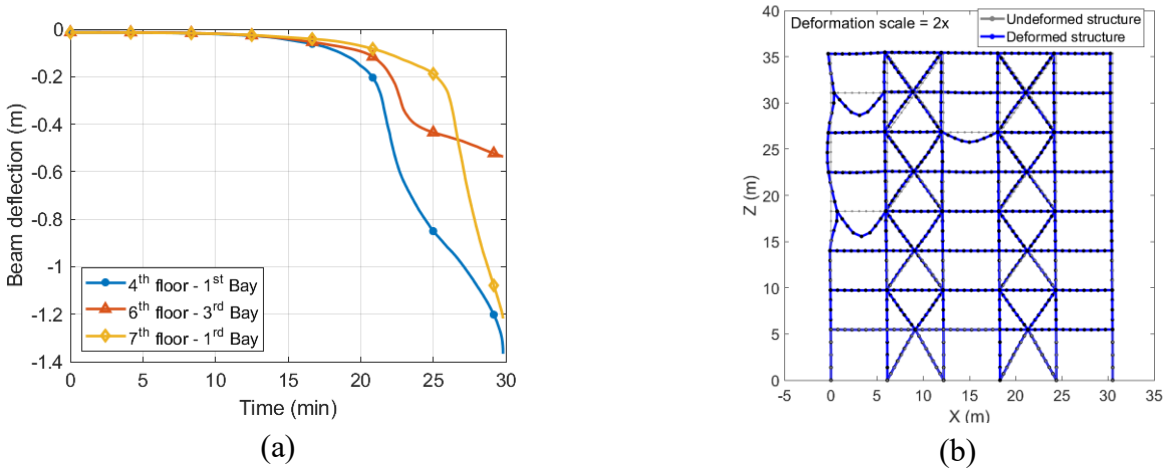

Figure 8. (a) Beams deflection (b) Deformed shape after 30 minutes (collapse).

4.3 Results

A total of 1680 simulations were performed for 14 accelerograms scaled at 6 different intensity values, 4 different values of window width, and 5 different fire load densities, as listed in Table 2. The Latin Hypercube Sampling (LHS) [30] was used to randomly generate the variable ε for steel retention factor $k_{y,2\%,T}$, which was needed to calculate the yield strength at ambient and high-temperatures for each simulation using Equation 1.

Table 2. Analysis parameters.

Parameter	**Values**
Accelerograms	14 accelerograms

Acceleration scale factor	0.50 0.75 1.00 1.25 1.50 1.75
Window width (m)	1.5 3.0 4.5 6.0
Fire load density (MJ/m^2)	300 600 900 1200 1500

Among the 1680 simulations, 1123 analyses did lead to an FFE event because either the PFA and IDR satisfied the three thresholds for an ignition to occur, as explained in the previous section. It is also worth noting that about 500 simulations did not lead to an FFE event because either the ground motion was not strong enough to ignite a fire in a compartment or the ground motion was too strong that caused the collapse of the structure owing to the seismic action. Finally, 43 of 1680 analyses were discarded because they were interrupted due to numerical problems in an early stage of the FFE simulation.

Figure 9a shows the number of ignitions as a function of the maximum Sa at the first period of the structure. It can be observed that for larger values of Sa the number of ignitions is higher. Figure 9b shows the number of ignitions as a function of the percentage of damaged walls and windows after the earthquake event.

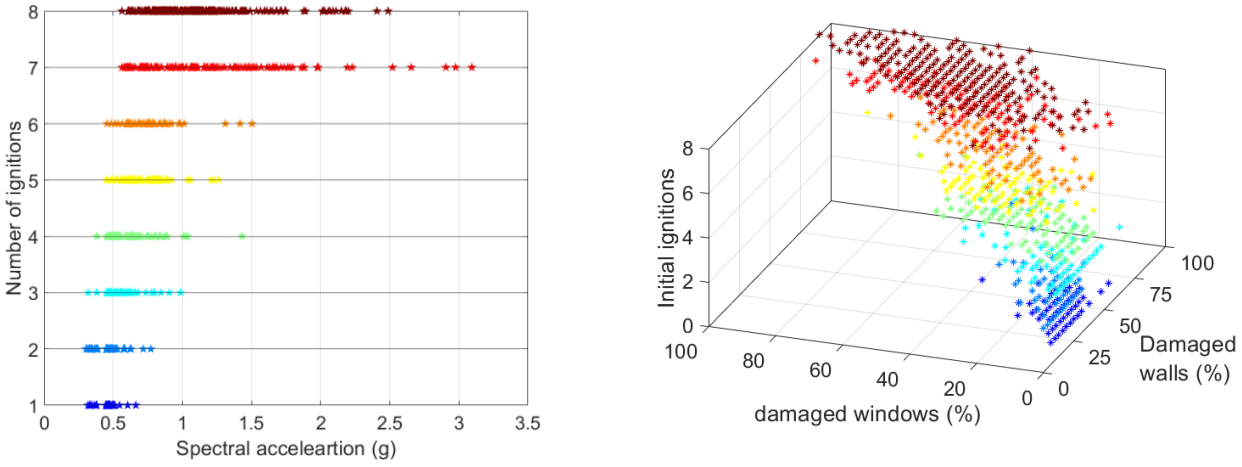

(a) (b)

Figure 9. (a) Number of ignitions vs Sa; (b) Number of ignitions vs damaged windows and walls.

4.4 Fragility functions

Based on the results of the FFE simulations, FFE fragility functions were developed in this section. A fragility function expresses the probability *P* of a given engineering demand parameter (EDP), such as IDR exceeding a certain limit state (LS) conditioned on an intensity measure (IM), such as peak ground acceleration or fire load density. Fragility functions are often expressed in terms of a lognormal cumulative distribution and have the form of Equation. 2.

$$P(EDP > LS|IM = x) = \emptyset\left(\frac{\ln\left(\frac{x}{\hat{\theta}}\right)}{\beta}\right) \qquad (2)$$

where $\emptyset$ is the standard normal cumulative distribution function (CDF), θ is the median of the IM and β is the standard deviation of the intensity measure. A typical EDP representing the damage induced by a seismic event is IDR, whereas in the case of an FFE, meaningful EDPs as related to structural fire engineering, such as vertical or horizontal displacements and displacement rates of structural members. A representative IM for an FFE scenario is the time to failure of a structural member that reflects the level of damage induced by the earthquake. Many researchers studied statistical procedures for estimating parameters of fragility functions and characterizing the results of probabilistic models, especially in the seismic domain [24-26] but also in the fire domain [27-29].Although the EDP is commonly assumed to follow a lognormal distribution when conditioned on the IM, several other distributions were considered

and compared using the Akaike information criterion (AIC) method [31,32], as illustrated in Figure 10. Equation 3 illustrates the AIC mathematical method, which evaluates and compares different possible statistical models and determines which one fits the data best.

$$AIC = -2 \ln L + 2k \tag{3}$$

where L and $\ln L$ are respectively the likelihood and the log-likelihood at its maximum point of the estimated model and k is the number of parameters. The use of a second-order corrected AIC (AICc) is recommended when the sample size is small compared to the number of parameters (n/k <40) [33], as shown in Equation 4:

$$AIC_c = AIC + \frac{2k^2 + 2k}{n - k - 1} \tag{4}$$

where n denotes the sample size. Note that for $n \to \infty$, $AIC_c = AIC$.

AIC uses a model maximum likelihood estimation (log-likelihood) as a measure of fit and adds a penalty term for models with higher parameter complexity to avoid overfitting. Given a set of candidate models for the data, the preferred model is the one with the minimum AIC value.

The outcome of the comparative analysis probability density function (PDF) and function distributions is illustrated in Figure 10. The results in Figure 10 indicate that compared to other statistical models, the lognormal distribution can serve as a candidate distribution to define the FFE fragility functions. However, the Generalized Extreme Value (GEV) distribution showed the best fit to the data.

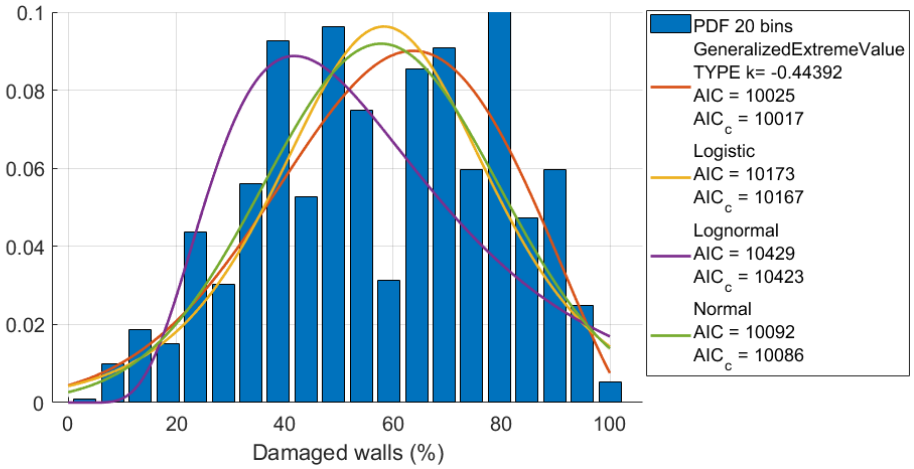

Figure 10. Probability density function (PDF) of the damaged walls and function distributions.

Based on the results of the comparative analysis, the GEV distribution was selected to derive the fragility functions. Not only the distribution provides the best fit, but also can be represented in a simple and closed form function with three parameters. The cumulative probability distribution function for the GEV distribution has the form of Eq 5.

$$P(EDP > LS|IM = x) = \begin{cases} \exp\left\{-\left[1 + k\left(\frac{x-\mu}{\sigma}\right)\right]^{-1/k}\right\} & if\ k \neq 0 \\ \exp\left\{-exp\left[-\left(\frac{x-\mu}{\sigma}\right)\right]\right\} & if\ k = 0 \end{cases} \tag{5}$$

where σ denotes the scale parameter (statistical dispersion of the probability distribution), μ is the location parameter (shift of the distribution) and k is the shape parameter. The shape parameter k is used to represent three different distribution families (Gumbel distribution, Fréchet distribution, reversed Weibull distribution). The shape value k is always below 0 for the case study analysed in this work (see Table 3). Thus, the GEV Type III was used for the fragility functions. This distribution is equivalent to the reversed Weibull distribution, whose tails are finite, such as the beta distribution.

Table 3. Parameters of the GEV and lognormal distribution for the damaged walls fragility functions and grouped based on S_a

	GEV distribution			Lognormal distribution	
	k	***σ***	***μ***	***σ***	***μ***
0.0 g < Sa ≤ 0.5 g	-0.209	11.89	25.26	0.492	3.306
0.5 g < Sa ≤ 1.0 g	-0.300	16.78	52.93	0.313	4.028
1.0 g < Sa ≤ 1.5 g	-0.535	13.78	75.37	0.183	4.345
1.5 g < Sa ≤ 2.0 g	-0.456	9.903	73.85	0.129	4.327
2.0 g < Sa ≤ 3.5 g	-0.166	7.400	76.03	0.102	4.367

Figure 11a and Figure 11b show the fragility curves for the damaged walls and grouped as a function of the Sa at the first period of the structure, respectively, using the GEV and Lognormal distribution. As expected, the Generalized Extreme Value (GEV) distribution showed a better fit to the data compared to the lognormal distribution.

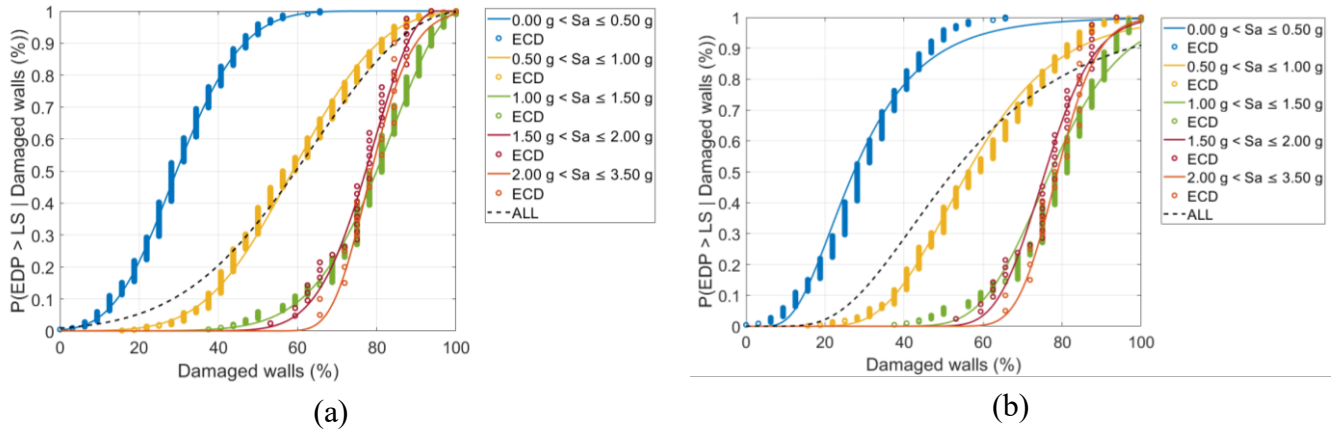

Figure 11. Empirical cumulative distribution (ECD) and fragility curves for the damaged walls as a function of Sa; (a): GEV distribution (b) Lognormal distribution.

Figure 12 shows the fragility curves for the partial collapse due to fire grouped as a function of the Sa at the first period of the structure.

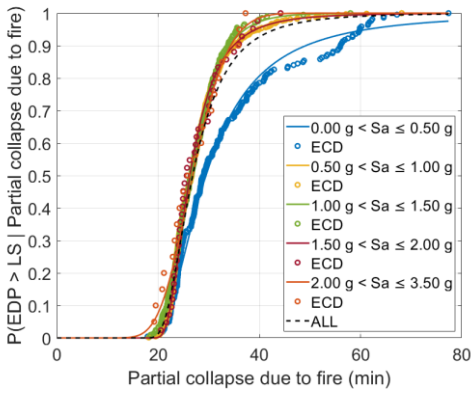

Figure 12. Empirical cumulative distribution (ECD) and fragility curves for the collapse state as a function of Sa

Figure 12 highlights a higher probability of exceedance of reaching partial collapse limit state with shorter times to collapse when the structure is subjected to higher values of spectral acceleration. In fact, at lower Sa values, there is a 90% probability of exceeding the partial collapse limit state in 49 minutes, whereas at higher Sa values, the partial collapse limit state is reached in 33 minutes.

5 CONCLUSIONS

The paper presented a methodology to perform fire following earthquake (FEE) analyses and described the development of a novel probabilistic FFE framework aimed at developing FFE fragility functions of a prototype steel braced frame. A decision tree algorithm was developed to establish the probability of ignition in the compartments within the building after the seismic event. Compartmentation and opening characteristics as well as the potential for fire spread were considered based on seismic damage in windows, doors, and partition walls following seismic fragility functions found in the literature.

The results showed that about 1123 analyses, out of 1680 randomly generated cases, experienced FFE events. The results of the probabilistic analyses were used to produce fragility functions to evaluate the probability of exceeding a damaged state conditioned on an intensity measure in the context of FFE. It was observed a higher probability of exceedance of reaching collapse limit state with shorter times to collapse when the structure is subjected to higher values of spectral acceleration. Moreover, higher values of the spectral acceleration tended to determine higher the number of ignitions. Although this study provided some insights on the performance of unprotected concentrically steel framed buildings subjected to the hazards of earthquake and fire, future research directions can include the study of other type of unprotected and protected steel structure, e.g., other braced frames and moment-resisting frames.

ACKNOWLEDGMENT

The support received from the Italian Ministry of Education, University and Research (MIUR) in the framework of the "Departments of Excellence" (grant L 232/2016) is gratefully acknowledged.

Computational support was provided by the Center for Computational Research at the University at Buffalo [34].

REFERENCES

1. Scawthorn C, Eidinger JM, Schiff AJ. (2005) "Fire following earthquake". Technical Council on Lifeline Earthquake Engineering Monograph, No. 26. American Society of Civil Engineers
2. Elhami-Khorasani N and Garlock MEM. (2017) "Overview of fire following earthquake: historical events and community responses", International Journal of Disaster Resilience in the Built Environment.
3. Botting, R. (1998). "The Impact of Post-Earthquake Fire on the Built Urban Environment". Fire Engineering Research Report 98/1, University of Canterbury, New Zealand.
4. Scawthorn C.R., Khater M. (1992). "Fire follow-ing Earthquake: Conflagration Potential in the in greater Los Angeles, San Francisco, Seattle and Memphis Areas", EQE International, pre-pared for the National Disaster Coalition, San Francisco, CA (available from the National Committee on Property Insurance, 75 Trem-ont, Suite 510, Boston, MA 02108-3910, (617. 722-0200]).
5. Covi, P. (2021). "Multi-hazard analysis of steel structures subjected to fire following earthquake", Doctoral dissertation, University of Trento. doi: 10.15168/11572_313383
6. McKenna, F. (2011). "Opensees: a framework for earthquake engineering simulation,"Computing in Science & Engineering, vol. 13, no. 4,pp. 58–66.
7. Elhami-Khorasani, N., Garlock, M. E., and Quiel, S. E. (2015). "Modeling steelstructures in opensees: Enhancements for fire and multi-hazard probabilistic analyses,"Computers & Structures, vol. 157, pp. 218–231.
8. Cadorin, J.F. and Franssen, J.M., (2003). A tool to design steel elements submitted to compartment fires—OZone V2. Part 1: pre-and post-flashover compartment fire model. Fire Safety Journal, 38(5), pp.395-427.
9. Federal Emergency Management Agency (FEMA). (2012). "Next-Generation Methodology for Seismic Performance Assessment of Buildings". Prepared by the Applied Technology Council for the Federal Emergency Management Agency, Report No. FEMA P-58, Washington, D.C.
10. MATLAB Release 2021b (2021), Natick, Massachusetts: The MathWorks Inc.
11. J. Ueno, S. Takada, Y. Ogawa, M. Matsumoto, S. Fujita, N. Has-sani, and F. S. Ardakani, (2004) "Research and development on fragility of components for the gas distribution system in greater Tehran, Iran,"Conferene Proceed-ings, in Proc. 13th WCEE, Vancouver, BCCanada, Paper, no. 193.

12. FEMA, (2000), “Prestandard and commentary for the seismic rehabilitation of buildings,”
13. Elhami -Khorasani, N., Gardoni, P., and Garlock M., (2015) “Probabilisticfire analysis: material models and evaluation of steel structuralmembers,”Journal of Structural Engineering, vol. 141, no. 12.
14. Qureshi, R., Ni, S., Elhami-Khorasani, N., Van Coile, R., Hopkin, D., and Gernay, T., (2020). “Probabilistic models for temperature-dependentstrength of steel and concrete,”Journal of Structural Engineering,vol. 146, no. 6, p. 04020102.
15. J. L. Harris and M. S. Speicher, (2015), “As-sessment of first generation performance-based seismic design methods for new steel buildings”. volume 2: Special concentrically braced frames .(national institute of standards and technology), NIST TechnicalNote, vol. 2, pp. 1863–2.
16. ASCE 7-10 (2010). “Minimum design loads for buildings and other structures”. American Society of Civil Engineers.[34] ASCE 7-10 (2010). “Minimum design loads for buildings and other structures”. American Society of Civil Engineers.
17. Federal Emergency Management Agency (FEMA) (2008): “FEMA P-695, Quantification of Building Seismic Performance Factors”.
18. Kircher, C., Deierlein, G., Hooper, J., Krawinkler, H., Mahin, S., Shing, B., and Wallace, J., (2010). “Evaluation of the fema p-695 method-ology for quantification of building seismic performance factors,”.
19. PEER 2013/03 “PEER NGA-West2 Database, by: Timothy D. Ancheta, Robert B. Darragh, Jonathan P. Stewart, Emel Seyhan, Walter J. Silva, Brian S.J. Chiou, Katie E. Wooddell, Rob-ert W. Graves, Albert R. Kottke, David M. Boore, Tadahiro Kishida, and Jennifer L. Do-nahue.”
20. CEN (2002): EN 1991-1-2 “Eurocode 1: Actions on structures - Part 1-2: General actions - Actions on structures exposed to fire”.
21. Elhami-Khorasani, N., Salado Castillo, J. G., Saula, E., Josephs, T., Nurlybekova, G., & Gernay, T. (2021). “Application of a digitized fuel load surveying methodology to office buildings”. Fire technology.
22. CEN (2005): EN 1993-1-2 “Eurocode 3: Design of steel structures - Part 1-2: General rules - Structural fire design”.
23. CEN (2005): EN 1993-1-1 “Eurocode 3: Design of steel structures - Part 1-1: General rules and rules for buildings”.
24. Baker, J. W. (2015). “Efficient analytical fragility function fitting using dynamic structural analysis”. Earthquake Spectra, 31(1), 579-599.
25. Calvi, G. M., Pinho, R., Magenes, G., Bommer, J. J., Restrepo-Vélez, L. F., and Crowley, H., (2006). “Development of seismic vulnerability assessment methodologies over the past 30 years”, ISET Journal of Earthquake Technology 43, 75–104.
26. Tondini, N., Zanon, G., Pucinotti, R., Di Filippo, R., & Bursi, O. S. (2018). “Seismic performance and fragility functions of a 3D steel-concrete composite structure made of high-strength steel”. Engineering Structures, 174, 373-383.
27. Lange, D., Devaney, S., & Usmani, A. (2014). “An application of the PEER performance based earthquake engineering framework to structures in fire”. Engineering Structures, 66, 100-115.
28. Gernay, T., Elhami-Khorasani, N., and Garlock, M., (2019). “Fire Fragility Functions for Steel Frame Buildings: Sensitivity Analysis and Reliability Framework,” Fire Technol., vol. 55, no. 4, pp. 1175–1210.
29. Randaxhe J., Popa N., Tondini N., (2021) “Probabilistic fire demand model for steel pipe-racks exposed to localised fires”, Engineering Structures, 226, 111310,
30. Olsson, A., Sandberg, G., and Dahlblom, O. (2003). “On Latin hypercube sampling for structural reliability analysis.” Structural Safety, 25(1), 47–68.
31. Akaike, H. (1998). Information theory and an extension of the maximum likelihood principle. In Selected papers of hirotugu akaike (pp. 199-213). Springer, New York, NY.
32. Akaike, H. (1974). “A new look at the statistical model identification”. IEEE transactions on automatic control, 19(6), 716-723.
33. Burnham, K. P., & Anderson, D. R. (1998). “Practical use of the information-theoretic approach”. In Model selection and inference (pp. 75-117). Springer, New York, NY.
34. Center for Computational Research, University at Buffalo, 2022. http://hdl.handle.net/10477/79221